11th International Conference on Through-life Engineering Services – TESConf2022
8-9 November 2022, Cranfield UK

Moment-Based Image Enhancement for Brain Tumor Health Monitoring

Barmak Honarvar Shakibaei Asli* and Yuhan Wang

Centre for Life-cycle Engineering and Management, Cranfield University, Cranfield, MK43 0AL, UK

* Corresponding author. Tel.: +44 (0) 1234 754128; *E-mail address: barmak@cranfield.ac.uk*

Abstract

Since the stable increasing incidence of brain tumors in recent years, brain tumor detection and monitoring are being attached with more importance. To implement the image feature extraction approach for the current imaging system, the image moments' concepts are introduced. The theory of image moments is applied for brain image analysis, which is a weighted average of the image pixels' intensities representing the characteristics of the mentioned brain images with potential tumor diseases. This paper describes several continuous and discrete moments in terms of the polynomial kernels used and distinguishes their differences regarding image reconstruction and enhancement. The experimental results confirm that the proposed discrete Tchebichef and Krawtchouk moments are more robust in terms of noise and blur reduction than the existing methods, such as the Wiener filter. This process explains how the proposed image moments technique can be applied in the health monitoring of brain tumors via image analysis procedures.

Keywords: Health monitoring; image moments; orthogonality; image enhancement; image analysis

1. Introduction

With the new generation of sensors and medical instruments, device producer companies can now drive health monitoring to a whole new level. In this regard, health sensing can be applied for point-of-care diagnostics, medical imaging, vital signs monitoring, and body disease monitoring.

The brain tumor is a disease in which abnormal cells form in the tissues of the brain cord [1], and brain tumors account for 85% to 90% of all primary central nervous system (CNS) tumors [2]. The cause of most adult brain tumors is unknown so far, and everyone's symptoms are different. Many different kinds of brain tumors are distinguished by the type of cell they formed in and where the tumor first forms like anaplastic astrocytomas and glioblastomas (see Fig. 1) (38% of primary brain tumors), Meningiomas and other mesenchymal tumors (27% of primary brain tumors), mixed glioma and so on.

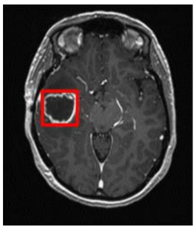

Fig. 1. Glioblastoma brain tumor.

Among all the brain tumors, Gliomas account for 70-80% of all [3,4]. Recently, the incidence rates of brain tumors have been rather stable, with a tendency for higher rates in highly developed, industrialized countries [5]. According to the statistics from the American Cancer Society, in 2021, brain tumors had become the most common adolescent cancer with a percentage of 21%, and also the second most common childhood cancer (27%) [6]. Therefore, deeper research into brain tumors with the newest technique is of great importance. Early detection of the brain tumor's location and shape clinic will be helpful in the treatment of the patient's disease. Medical imaging techniques are developed with the increasing requirements for fast and accurate medical diagnosis. It refers to processes used to create images of the human body for various clinical purposes such as medical procedures and diagnosis or medical science including the study of normal anatomy and function [7]. As for brain imaging, the most popular studies are Magnetic Resonance Imaging (MRI) and Computed Tomography (CT) [8], which have been widely used in real life (see Figs. 2 and 3 for MRI and CT brain tumor examples). Due to the requirements for faster and earlier health monitoring, medical imaging is developing rapidly. It aims at creating clear images inside the human body for detection, and as for brain images, the most popular studies are MRI and CT [9,10]. MRI scanners use magnetic fields and radio waves to generate clear images of organs, especially soft tissues, while CT relies on X-ray technology and is more sensitive to density changes so that it detects bone structures near the brain tumor more precisely.

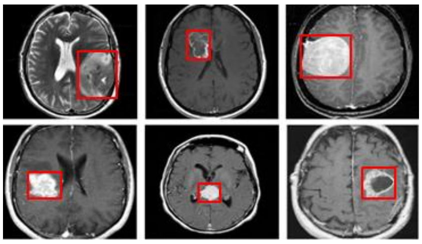

Fig. 2. MRI brain tumor images.

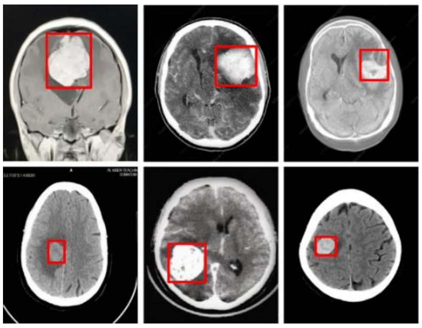

Fig. 3. CT brain tumor images.

Moment-based image analysis is a quickly developing area [11], in which a polynomial representing the image is used for processing, such as enhancement. In this paper, we propose a moment-based analysis for active brain tumor health monitoring. By using moment and moment invariant theories, it is possible to achieve relevant information about images. However, there are several continuous and discrete moments for image study. We recall Legendre, Chebyshev, and Zernike moments as continuous types and discuss Tchebichef and Krawtchouk moments for the discrete case [12,13,14,15]. The orthogonality property of the mentioned moments would help this research to prevent redundant information and their sensitivity to noise.

The remainder of this paper is organised as follows. In section 2, some continuous and discrete moment functions are reviewed as the proposed framework. Section 3 presents the moment-based analysis for brain tumor health monitoring. Some experimental results for enhancing the brain tumor images using moment theories are discussed in Section 4, and Conclusions are given in Section 5.

2. Method

With the development of computer technology, the application of image processing in the medical area became a hot spot. Medical image processing is a process to highlight important information contained in Brain tumor images (no matter MRI or CT). To extract information effectively, the conception Moment is proposed during processing.

Moments are projections of the image onto a polynomial basis. To improve the applicability of moments, moment invariants are introduced in 1961 by Hu [16] including scale-invariant, translation-invariant, and rotation-invariant. The Geometric moment (GM) for a two-dimensional (2D) function $f(x,y)$ of order $(p+q)$ is a very basic moment which is defined as:

$$M_{pq} = \iint_{-\infty}^{+\infty} x^p y^q f(x,y)dxdy \tag{1}$$

where $p,q = 0,1,2,\dots,\infty$. From GM, simple image properties are derived, including the sum of grey level when $p = q = 0$, centroid location when $p + q = 1$, and so on. The centroid location given by GM has been applied for defining the coordinate circle centers to minimalize misconceptions about full perfect circles and has been proved to be faster than the former method [17]. GM's basic set $\{x^p y^q\}$ is complete, but not orthogonal. Central moments are defined as:

$$\mu_{pq} = \iint_{-\infty}^{+\infty} (x-\bar{x})^p (y-\bar{y})^q f(x,y)dxdy \tag{2}$$

where $\bar{x}$ and $\bar{y}$ are the components of the centroid. Central moments are translational invariant.

The orthogonal moments are firstly introduced by Teague in 1980 [18]. It is a special category of moments, which helps recover the image from moments. In past decades, many different orthogonal moments are proposed in continuous form, i.e. Legendre Moments (LMs) and Chebyshev moments (CMs) [14,19]. By the orthogonality principle, the image function $f(x,y)$ can be written as an infinite series [20] in terms of each moment's polynomials (see Appendix A for the definitions of the Legendre and Chebyshev polynomials).

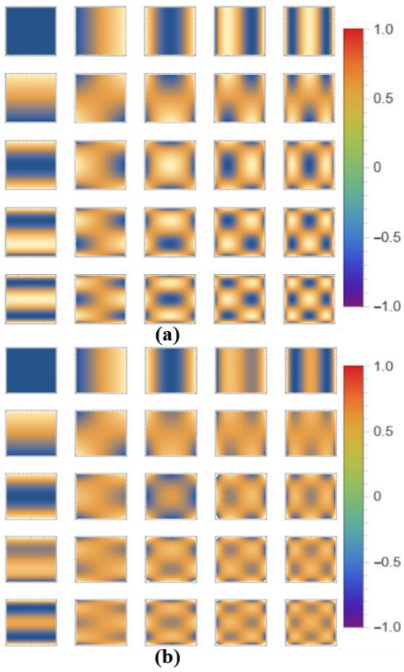

Fig. 4. The graphs of 2D kernel functions of: (a) the LMs and (b) CMs of the first kind up to the fourth degree.

The kernel functions of the 2D LMs and CMs on $\langle -1,1 \rangle \times \langle -1,1 \rangle$ are shown in Fig. 4. On the other hand, the discrete moments are more suitable for digital image analysis since no mapping is needed for digital coordinates. Two significant types of discrete moments are Tchebichef and Krawtchouk moments (TMs and KMs) [21,22]. The 2D Tchebichef and Krawtchouk moments are defined as follows, respectively:

$$T_{nm} = \sum_{x=0}^{N-1} \sum_{y=0}^{N-1} t_n(x) t_m(y) f(x,y) \tag{3}$$

$$K_{nm} = \sum_{x=0}^{N-1} \sum_{y=0}^{N-1} k_n(x;p) k_m(y;p) f(x,y) \tag{4}$$

where $n, m, x, y = 0,1,2, \dots, N-1$, N is the size of the image and $p \in (0,1)$ (see Appendix A for the exact definitions of the Tchebichef and Krawtchouk polynomials). Fig. 5 shows the kernel functions of the 2D TMs and KMs for $N = 5$ and $p = 1/2$. Compared to the Tchebichef moment, the Krawtchouk moment performs better in extracting local features of an image [22]. So far, Tchebichef and Krawtchouk moments are applied for many different kinds of image processing. Firstly, they are combined with Hahn moment to be an effective image classification tool [23]. They are also proved to be suitable for segmentation [24]. Due to the orthogonal characteristic, image reconstruction is also achievable [25].

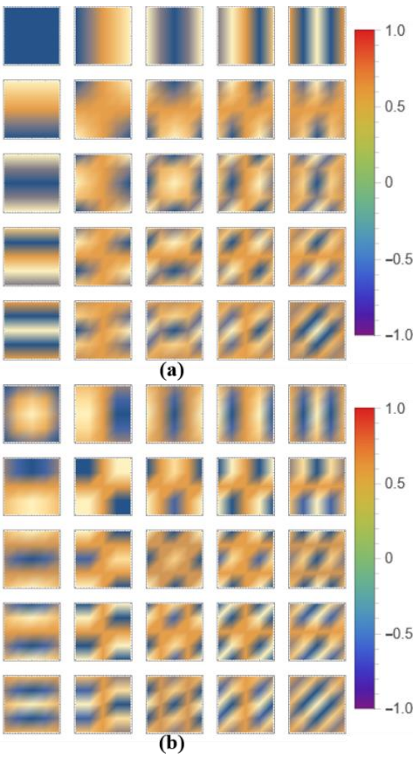

Fig. 5. The graphs of 2D kernel functions of: (a) the TMs and (b) KMs up to the fourth degree.

3. Moment-based image enhancement

If the original image is assumed as $f(x,y)$, the degraded image $g(x,y)$ can be expressed in the following form:

$$g(x,y) = h(x,y) * f(x,y) + n(x,y) \tag{5}$$

where $*$ denotes the 2D convolution, $h(x,y)$ is the space-variant point spread function (PSF) describing the response of an imaging system to point source/object, and $n(x,y)$ is the noise. The image degradation and restoration model is shown in Fig. 6. For MRI medical images, the most common noise type is Rician noise, in other words, the image is Rician distributed, which can be degraded as a combination of Rayleigh distribution and Gaussian distribution, but not an additive noise.

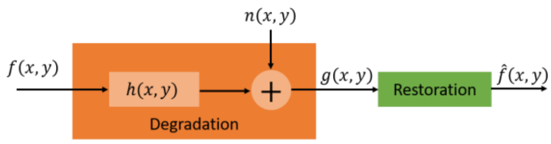

Fig. 6. Image degradation and restoration model.

Since the degradation model is simulated as a convolution process, in traditional restoration methods the image restoration will be a deconvolution process so that filtering is directly applied to degraded images. However, for moment-based methods, images are firstly projected to a polynomial system. The polynomials are then dealt with inverse filtering to get restored functions, and then they are reconstructed to final restored images. By extracting polynomials from images, the effects of noise will be decreased, making inverse filtering more possible to restore the polynomials to the original ideal version. Fig. 7 shows the image reconstruction process using the extracted TMs or KMs after applying a suitable inverse filter to remove any blur or noise.

Fig. 7. Image reconstruction process using TMs and KMs techniques.

4. Experimental results

To prove the validity of moment-based image analysis methods, we have conducted several controlled experiments to compare the performance of traditional filters and moment-based methods. To evaluate the quality of restored images, Image Quality Assessments (IQA) methods are applied. In this paper, we mainly use Full Reference-IQA (FR-IQA) and No reference-IQA (NR-IQA) techniques. The other approaches such as the structural similarity index measure (SSIM) require an original image as a

Table 1. TMs and KMs filtering results for the clinical MRI brain tumor images compared to classical Gaussian and Wiener filters. The last two columns show that the proposed methods are performing the restoration process better than both filters.

Original Image	Gaussian Filter	Wiener Filter	TMs method	KMs method
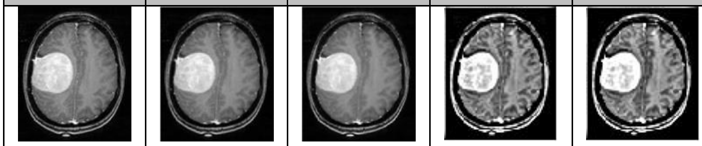				
BRISQUE	31.6498	30.1944	**27.1873**	**25.0341**
PIQE	49.9357	32.0595	**26.9519**	**23.7702**
NIQE	4.2062	4.6019	**3.3302**	**2.8932**
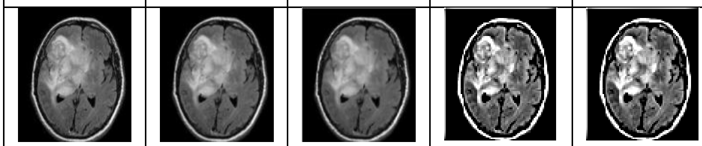				
BRISQUE	43.5768	42.5055	**37.6051**	**32.4392**
PIQE	51.1344	31.7674	**29.9713**	**25.5011**
NIQE	6.9216	8.0798	**5.9319**	**4.0341**
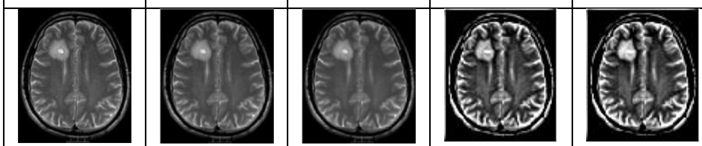				
BRISQUE	41.2946	39.6769	**34.2395**	**29.0056**
PIQE	61.3180	35.7334	**27.7843**	**22.0321**
NIQE	5.2460	5.3030	**4.1299**	**4.0831**
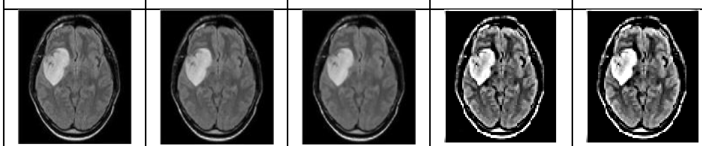				
BRISQUE	41.8754	45.6561	**38.8551**	**37.9016**
PIQE	56.3133	34.7749	**30.5569**	**28.9143**
NIQE	7.5361	8.1796	**6.7705**	**6.0015**
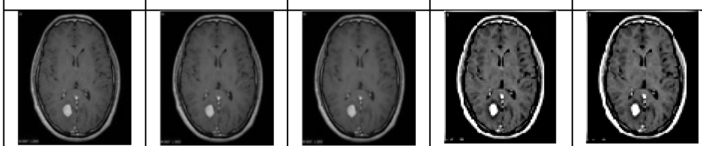				
BRISQUE	49.2882	34.0210	**29.4762**	**26.3408**
PIQE	55.4373	35.8451	**31.5774**	**28.9461**
NIQE	8.3397	9.7096	**6.7881**	**5.3945**

Table 2. TMs and KMs filtering results for the clinical CT brain tumor images compared to classical Gaussian and Wiener filters. The last two columns show that the proposed methods are performing the restoration process better than both filters.

Original Image	Gaussian Filter	Wiener Filter	TMs method	KMs method
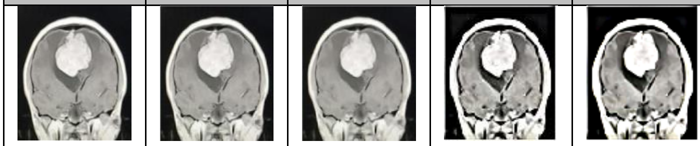				
BRISQUE	27.4331	30.9072	**25.5688**	**22.7612**
PIQE	63.4046	73.0544	**57.8902**	**51.3345**
NIQE	4.2643	4.9033	**3.7639**	**3.0134**
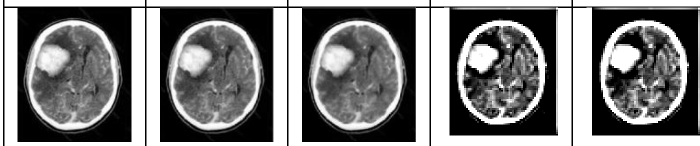				
BRISQUE	34.0337	38.5810	**31.9635**	**28.6604**
PIQE	49.6907	60.3500	**42.8752**	**37.0066**
NIQE	3.8223	4.2682	**3.3385**	**2.9873**
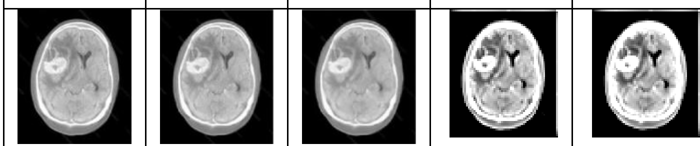				
BRISQUE	46.8093	47.8089	**39.7661**	**38.0559**
PIQE	51.3441	63.4789	**44.7739**	**41.9744**
NIQE	7.4663	7.3201	**6.5033**	**5.8877**
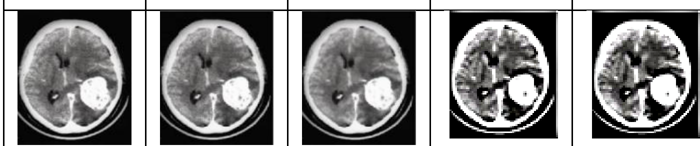				
BRISQUE	38.2605	41.7947	**35.5682**	**31.7739**
PIQE	50.3818	68.6602	**46.9322**	**40.0032**
NIQE	3.8731	4.7436	**3.5454**	**3.1169**
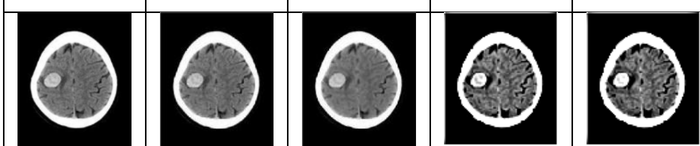				
BRISQUE	35.4152	36.4903	**30.8734**	**28.8744**
PIQE	38.7768	44.7528	**34.4099**	**31.5981**
NIQE	9.6442	9.3900	**7.2947**	**7.0008**

reference to measure the test image, whereas the NR-IQA only requires images that need to be measured by themselves. The blind/reference-less image spatial quality evaluator (BRISQUE) is applied to get a score for image measurement from a natural image model [26,27]. The score measures the image quality by using the locally normalized luminance coefficients, which were used to calculate the image features. For this score, a lower value indicates better subjective quality. Two more criteria as no-reference image quality scores are Perception-based Image Quality Evaluator (PIQE) and Naturalness Image Quality Evaluator (NIQE). For PIQE and NIQE metrics, the lower scores represent a better image quality as well as BRISQUE.

We perform two different experiments to show the moment-based method's robustness compared to the state-of-the-art techniques, i.e. Gaussian and Wiener filtering. These approaches provide filtering performances for complex structure images and large noise variance. As the result of the first experiment, which has been done for a set of brain MRI images, Table 1 illustrates the superiority of the TMs and KMs methods compared to the Gaussian and Wiener filtering techniques. The NR-IQA could help us to distinguish the image quality after the image restoration process. The TMs and KMs approaches have the lowest scores of NR-IQA standards. This means we can use TMs/KMs-based image reconstruction to improve the MRI imaging system for brain tumor health monitoring mechanisms.

In the second experiment, which uses several CT brain images, we use the TMs and KMs to restore other brain tumor images. The comparison has been performed using the same Gaussian and Wiener filtering methods. As can be seen from Table 2, the last two columns show a significant improvement in image reconstruction using TMs and KMs. However, both tables are a good comparison between the enhanced MRI/CT brain images using two moment-based proposed algorithms. By comparing the last two columns of both tables, it can be seen the KMs are performing better image improvement than the TMs in terms of the IQA results. Both TMs and KMs are discrete orthogonal moments and matched with the nature of digital images, while the LMs and CMs are suitable for 2D continuous signals because of their continuity properties of the Legendre and Chebyshev polynomials.

5. Conclusion

In this paper, different types of moments are discussed to distinguish their application in the continuous and discrete domain systems and introduce how they are set as the kernel function for image analysis in brain tumor health monitoring. Legendre moments and Chebyshev moments are continuous moments, while the discrete Tchebichef and Krawtchouk polynomials can be applied to digital images as discrete moments. Moreover, the moments' definitions are explained, and then we demonstrate how the orthogonal moments can be applied in brain tumor images to extract the information and features of tumors. We compare the image enhancement results as restoration and reconstruction using different moments with the existing techniques such as the Wiener filter to show their advantages and accuracies in the medical imaging systems. With further development of computer technology and moment theory, it is predicted that moment-based image analysis will be more effective.

Appendix A

A.1 Legendre polynomials:

$$P_n(x) = \frac{1}{2^n n!}\frac{\mathrm{d}^n}{\mathrm{d}x^n}(x^2-1)^n \qquad \text{(A.1)}$$

A.2 Chebyshev polynomials of the first kind:

$$T_n(x) = \frac{1}{2}\left[\left(x-\sqrt{x^2-1}\right)^n + \left(x+\sqrt{x^2-1}\right)^n\right] \qquad \text{(A.2)}$$

A.3 Discrete Tchebichef polynomials:

$$t_n(x) = (1-N)_n \, {}_3F_2(-n,-x,1+n;1,1-N;1) \qquad \text{(A.3)}$$

where ${}_pF_q$ is the hypergeometric function, and $(a)_k$ is the Pochhammer symbol defined by:

$$(a)_k = a(a+1)(a+2)\ldots(a+k-1)$$

A.4 Krawtchouk polynomials:

$$k_n(x;p,N-1) = {}_2F_1(-n,-x;1-N;\tfrac{1}{p}) \qquad \text{(A.4)}$$

References

[1] P. D. Q. A. T. E. Board, "Adult central nervous system tumors treatment (PDQ®)," in *PDQ Cancer Information Summaries [Internet]*, National Cancer Institute (US), 2021.

[2] P. Kleihues and W. K. Cavenee, "Pathology and genetics of tumours of the nervous system. International Agency for Research on Cancer," *World Heal. Organ. Lyon, Fr.*, 2000.

[3] B. K. Ahir, H. H. Engelhard, and S. S. Lakka, "Tumor development and angiogenesis in adult brain tumor: glioblastoma," *Mol. Neurobiol.*, vol. 57, no. 5, pp. 2461–2478, 2020.

[4] H. Ohgaki, "Epidemiology of brain tumors," *Cancer Epidemiol.*, pp. 323–342, 2009.

[5] H. Ohgaki and P. Kleihues, "Epidemiology and etiology of gliomas," *Acta Neuropathol.*, vol. 109, no. 1, pp. 93–108, 2005.

[6] R. L. Siegel, K. D. Miller, H. E. Fuchs, and A. Jemal,

"Cancer statistics, 2021," *Ca Cancer J Clin*, vol. 71, no. 1, pp. 7–33, 2021.

[7] D. Ganguly, S. Chakraborty, M. Balitanas, and T. Kim, "Medical imaging: A review," in *International Conference on Security-Enriched Urban Computing and Smart Grid*, 2010, pp. 504–516.

[8] S. Parisot, "Understanding, Modeling and Detecting Brain Tumors: Graphical Models and Concurrent Segmentation/Registration methods." Ecole Centrale Paris, 2013.

[9] "CT scan - Wikipedia." https://en.wikipedia.org/wiki/CT_scan (accessed Sep. 26, 2022).

[10] "Magnetic resonance imaging - Wikipedia." https://en.wikipedia.org/wiki/Magnetic_resonance_imaging (accessed Sep. 26, 2022).

[11] C. Höschl, "Advanced Moment-Based Methods for Image Analysis," 2018.

[12] B. H. S. Asli and J. Flusser, "Fast computation of Krawtchouk moments," *Inf. Sci. (Ny).*, vol. 288, pp. 73–86, 2014.

[13] B. Honarvar Shakibaei Asli, R. Paramesran, and C. L. Lim, "The fast recursive computation of Tchebichef moment and its inverse transform based on Z-transform," *Digit. Signal Process. A Rev. J.*, vol. 23, no. 5, 2013, doi: 10.1016/j.dsp.2013.05.004.

[14] C.-L. Lim, B. Honarvar, K.-H. Thung, and R. Paramesran, "Fast computation of exact Zernike moments using cascaded digital filters," *Inf. Sci. (Ny).*, vol. 181, no. 17, pp. 3638–3651, 2011.

[15] K. M. Hosny, A. M. Khalid, and E. R. Mohamed, "Efficient compression of volumetric medical images using Legendre moments and differential evolution," *Soft Comput.*, vol. 24, no. 1, pp. 409–427, 2020.

[16] M.-K. Hu, "Visual pattern recognition by moment invariants," *IRE Trans. Inf. theory*, vol. 8, no. 2, pp. 179–187, 1962.

[17] R. Fachruddin and J. L. Buliali, "Circle Detection System Using Image Moments," in *2022 IEEE International Conference on Cybernetics and Computational Intelligence (CyberneticsCom)*, 2022, pp. 265–269.

[18] M. R. Teague, "Image analysis via the general theory of moments," *Josa*, vol. 70, no. 8, pp. 920–930, 1980.

[19] E. H. Doha, "The first and second kind Chebyshev coefficients of the moments for the general order derivative on an infinitely differentiable function," *Int. J. Comput. Math.*, vol. 51, no. 1–2, pp. 21–35, 1994.

[20] C.-H. Teh and R. T. Chin, "On image analysis by the methods of moments," *IEEE Trans. Pattern Anal. Mach. Intell.*, vol. 10, no. 4, pp. 496–513, 1988.

[21] R. Mukundan, S. H. Ong, and P. A. Lee, "Image analysis by Tchebichef moments," *IEEE Trans. image Process.*, vol. 10, no. 9, pp. 1357–1364, 2001.

[22] P.-T. Yap, R. Paramesran, and S.-H. Ong, "Image analysis by Krawtchouk moments," *IEEE Trans. image Process.*, vol. 12, no. 11, pp. 1367–1377, 2003.

[23] A. Hmimid, M. Sayyouri, and H. Qjidaa, "Image classification using a new set of separable two-dimensional discrete orthogonal invariant moments," *J. Electron. Imaging*, vol. 23, no. 1, p. 013026, 2014.

[24] M. Tuceryan, "Moment-based texture segmentation," *Pattern Recognit. Lett.*, vol. 15, no. 7, pp. 659–668, 1994.

[25] B. Honarvar, R. Paramesran, and C.-L. Lim, "Image reconstruction from a complete set of geometric and complex moments," *Signal Processing*, vol. 98, pp. 224–232, 2014.

[26] A. Mittal, A. K. Moorthy, and A. C. Bovik, "No-reference image quality assessment in the spatial domain," *IEEE Trans. image Process.*, vol. 21, no. 12, pp. 4695–4708, 2012.

[27] N. Venkatanath, D. Praneeth, M. C. Bh, S. S. Channappayya, and S. S. Medasani, "Blind image quality evaluation using perception based features," in *2015 Twenty First National Conference on Communications (NCC)*, 2015, pp. 1–6.